Graphical Abstract

Intrinsic sodium regulation by Na,K-ATPase: The blue crab's salinity adaptation described by a single negative feedback loop

Peter Ruoff

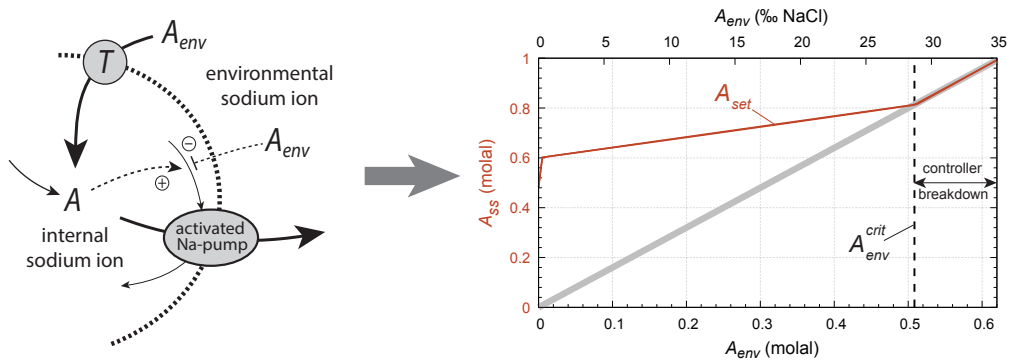

pump-based feedback

homeostatic behavior

Highlights

Intrinsic sodium regulation by Na,K-ATPase: The blue crab's salinity adaptation described by a single negative feedback loop

Peter Ruoff

- The salt adaptation of the blue crab has been investigated based on an internal negative feedback by the sodium pump.
- While the salt adaptation of the blue crab has been a defining example of *enantiostasis* the present results indicate that the blue crab's salt adaptation is a homeostatic property based on an internal feedback in the pump's Albers-Post mechanism.
- The results further suggest that other pumps based on the Albers-Post mechanism may contain similar negative feedbacks and thereby contribute to homeostatic regulation.

Intrinsic sodium regulation by Na,K-ATPase: The blue crab's salinity adaptation described by a single negative feedback loop

Peter Ruoff

University of Stavanger, Department of Chemistry, Bioscience, and Environmental Engineering, Kjell Arholms gate 41, Stavanger, 4021, Rogaland, Norway

---

Abstract

The term *enantiostasis* was introduced by Mangum and Towle to describe functional relationships between environmental changes and an organism's adaptation to them, and furthermore, to distinguish this kind of adaptation from homeostatic control. The defining example of enantiostasis is the blue crab's blood salinity response when exposed to different environmental salinities during the organism's move between the ocean and upriver freshwater conditions. In this paper an internal negative feedback loop in the Albers-Post mechanism of the sodium pump (Na,K-ATPase, NKA) is used to describe the blue crab's salinity adaptations. The following assumptions are made: Internal sodium ion activates NKA, while external sodium ion inhibits it. To describe the pump's behavior on changed environmental salinities, integral control is implemented by assuming that the activated pump is deactivated by zero-order or close to zero-order kinetics. As a result, internal sodium ion is robustly regulated by the feedback's environmentally changing setpoint. Enantiostasis and the closely related concept of rheostasis were both introduced to distinguish them from homeostatic mechanisms. However, the here presented results suggest that enantiostasis and the related rheostatic setpoint changes can be viewed as the emergence from a single homeostatic feedback regulation. In addition, the here suggested intrinsic negative feedback of NKA may be present in other Albers-Post based pumps and may also there contribute to homeostatic regulation.

Keywords: Enantiostasis, rheostasis, homeostasis, integral control, robust perfect adaptation, windup, Na,K-ATPase, sodium pump

1. Introduction

One of the essential features of organisms is their ability to adapt to changed environmental and anticipated conditions. Homeostasis, a concept coined by Walter Cannon in 1929, is a central adaptation strategy by keeping most of an organism's steady states within relative narrow limits (Cannon, 1929; Langley, 1973; Clancy and McVicar, 2002). However, there are apparently other strategies. Mangum and Towle (1977) introduced the term 'entantiostasis' to highlight an adaptation strategy with a *conserved functional relationship* between the changing environment and the organism's internal steady states (Hochachka and Somero, 1984). As an illustrative and defining example for this kind of adaptation Fig 1 shows how blood osmolality in the blue crab *Callinectes sapidus* changes as the animal encounters different environmental salinities which range from saltwater (35 ‰ or even higher) to fresh water (Mangum and Towle, 1977). Since the slope in blood osmolality between 1 ‰ to about 27 ‰ is significantly greater than zero, Mangum and Towle conclude that this type of adaptation is opposite to homeostatic, i.e. enantiostatic.

In this paper the author shows that the adaptation response in Fig 1 can be understood by an intrinsic negative feedback mechanism of the Na,K-ATPase (NKA) pump. Although the osmolality setpoint is changed in a rheostatic manner (Mrosovsky, 1990; Stevenson, 2024), its regulation is homeostatic and is able to show robust perfect adaptation. The relationship between enantatiostasis, rheostasis, and homeostasis is discussed at the end of the paper showing that the enantiostatic and rheostatic responses of the blue crab's salinity adaptation are an emergent homeostatic property. The results further suggest that other pump mechanisms based on the Albers-Post scheme may contain similar intrinsic negative feedback loops.

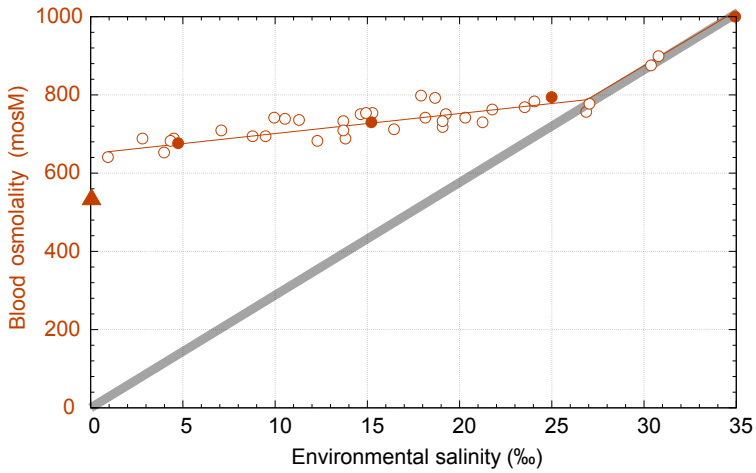

Figure 1: Defining enantiostasis: Blood osmotic concentration as a function of environmental salinity in the blue crab. Open circles represent values of caught animals in various salinities. The triangle is the average of crabs caught in freshwater. Solid dots represent mean values of crabs acclimated at different salinities in the laboratory. The grey thick diagonal has been described by Mangum and Towle (1977) as an isosmotic line. Redrawn from Fig 2 of Mangum and Towle (1977).

2. Materials and methods

2.1. Calculations and graphical presentations

Computations were performed with the Fortran subroutine LSODE (Radhakrishnan and Hindmarsh, 1993). Gnuplot (`www.gnuplot.info`) was used to generate figures, while reaction schemes and plot annotations were prepared with Adobe Illustrator (`www.adobe.com`). A set of Python scripts are provided for documentation (see Supporting Material).

2.2. Negative feedback motif and implementation of integral control

Fig 2 shows the negative feedback structure to describe Fig 1. It is based on one of eight earlier suggested negative feedback motifs (M1-M8) (Drengstig et al., 2012). The reason for choosing this motif (M5) is that it matches the main regulations of the Na-K ATPase (NKA), which is a central regulator of the blood sodium concentration in the blue crab.

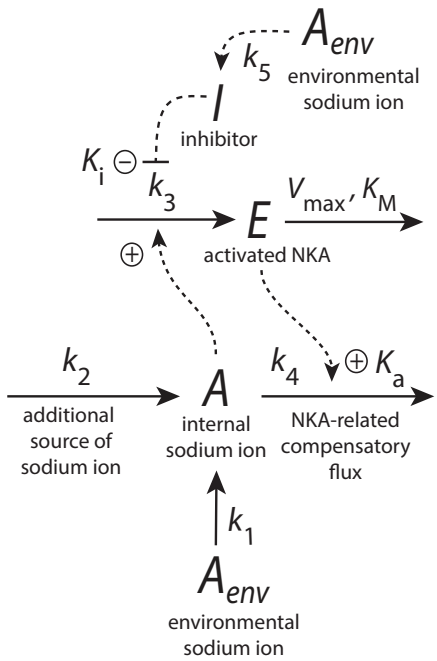

Figure 2: Negative feedback model (motif 5, Drengstig et al. (2012)) to describe blood sodium regulation displayed in Fig 1. The controlled variable A refers to the internal blood sodium ion concentration. Internal sodium ion activates the sodium pump (Kaplan, 1982; Skou and Esmann, 1992) by help of ATP and enables the extrusion of sodium ion into the environment. In the model the activated NKA is described as E, which plays the role of the controller (manipulated) variable. There are two inflows to A, one from A_{env} (environmental sodium ion) and the other from sources when the crab lives in freshwater. Environmental sodium ion is known to inhibit NKA (Garrahan and Glynn, 1967; Sachs, 1977; Kaplan, 1982). In the model this is implemented by A_{env} inducing I, which inhibits the activation of the pump. K_a and K_i are activation and inhibition constants, respectively.

The model is considered as follows. The controlled variable A is the internal (blood) sodium ion concentration. Environmental sodium ion (A_{env}) flows into the blood stream with rate constant k_1. There is also an additional constitutive sodium ion source via rate constant k_2, which becomes of importance when crabs live in freshwater. All sodium ion concentrations are in molality (m, number of mol Na per 1000g water) or are recalculated in ‰ NaCl solution. Concentrations of activated pump E, inhibitor I, and time scale are in arbitrary units.

The rate equations are:

$$\dot{A} = k_1 \cdot A_{env} + k_2 - \underbrace{k_4 \cdot A \overbrace{\left(\frac{E}{K_a + E}\right)}^{\text{activation term}}}_{\text{compensatory flux}} \tag{1}$$

$$\dot{E} = k_3 \cdot A \underbrace{\left(\frac{K_i}{K_i + I}\right)}_{\text{inhibition term}} - V_{max} \left(\frac{E}{K_M + E}\right) \tag{2}$$

In addition, the sensed fraction of A_{env} which causes inhibition, I, is considered to be proportional to A_{env}, i.e.

$$I = k_5 \cdot A_{env} \tag{3}$$

In integral control, a method from control engineering (Wilkie et al., 2002), the error of the controlled variable (i.e. the difference between the actual value of the controlled variable and its setpoint) is integrated, which then is fed back to regulate the controlled variable. This type of regulation leads to robust perfect adaptation (Yi et al., 2000; Khammash, 2021) where the controlled variable is moved precisely to its setpoint.

Integral control can be implemented by several kinetic approaches (Yi et al., 2000; Ni et al., 2009; Drengstig et al., 2012; Shoval et al., 2010; Briat et al., 2016; Fjeld et al., 2017; Aoki et al., 2019; Waheed et al., 2022). Here we use a process/enzyme, which removes or transports the controller variable E out of the negative feedback loop and works under zero-order or near zero-order conditions with respect to E, such that $E/(K_M + E) \approx 1$ (Ni et al., 2009). At steady state, Eq 2 then defines A's setpoint at $A_{set} = (V_{max}/k_3) \cdot (1 + I/K_i)$:

$$\dot{E} = k_3 \cdot A_{ss} \cdot f_i - V_{max} \underbrace{\left(\frac{E}{K_M + E}\right)}_{\approx 1} = -k_3 f_i \underbrace{\left(\underbrace{\left(\frac{V_{max}}{k_3 f_i}\right)}_{A_{set}} - A_{ss} \right)}_{error} = 0 \tag{4}$$

with f_i=$K_i/(K_i$+$I)$.

For small enough K_M values A_{ss} is practically at A_{set} (see Results), but the error increases as K_M increases (Drengstig et al., 2012). As required by integral control, Eq 4 shows that the concentration of E (the activated sodium pump) becomes proportional to the integrated error when zero-order condition is applied.

2.3. Controller breakdown

As A rises by increased A_{env} levels the compensatory flux in Eq 1 rises concomitantly by higher induced E values, which keeps A at A_{set}. The compensatory flux reaches its limits when the activation term goes into saturation, i.e. $E/(K_a$+$E)\approx 1$. This is the begin of controller breakdown since the negative feedback will not be able to keep A at A_{set} with A_{env} further increasing. The critical A_{env} concentration when controller breakdown starts to occur can be estimated by setting in Eqs 1 and 2 A_{env}=A_{env}^{crit}, A_{ss}=A_{set}, and $E/(K_a$+$E)$=1. This leads to the equations

$$\dot{A} = k_1 \cdot A_{env}^{crit} + k_2 - k_4 \cdot A_{set} = 0 \tag{5}$$

and

$$\dot{E} = k_3 \cdot A_{set} \left(\frac{K_i}{K_i + k_5 A_{env}^{crit}} \right) - V_{max} = 0 \tag{6}$$

Solving for A_{set} from Eq 6 and inserting it into Eq 5 gives, after some algebra, the expression for A_{env}^{crit}

$$A_{env}^{crit} = \frac{K_i(k_4 V_{max} - k_2 k_3)}{k_1 k_3 K_i - k_4 k_5 V_{max}} \tag{7}$$

When A_{env} is kept constant k_1 or k_2 can be changed while still keeping A_{ss} at A_{set}. Controller breakdown starts to occur when compensatory flux becomes saturated when k_1 exceeds k_1^{crit} or when k_2 exceeds k_2^{crit} with

$$k_1^{crit} = \frac{k_4 \cdot A_{set} - k_2}{A_{env}} \tag{8}$$

$$k_2^{crit} = k_4 \cdot A_{set} - k_1 \cdot A_{env} \tag{9}$$

3. Results

Fig 3 shows A in dependence of A_{env} when a set of rate constant values were used to mimic the experimental behavior in Fig 1. Note that these values are not unique, i.e. other combinations are possible which would lead to the same behavior as described in panel a. As long as $A_{env}<A_{env}^{crit}$ the controller is operative and $A_{ss}=A_{set}$ (Eq 4). The slight positive slope of the red A_{ss} ($=A_{set}$) line is due to the increased inhibitor concentration as A_{env} increases (Eq 3).

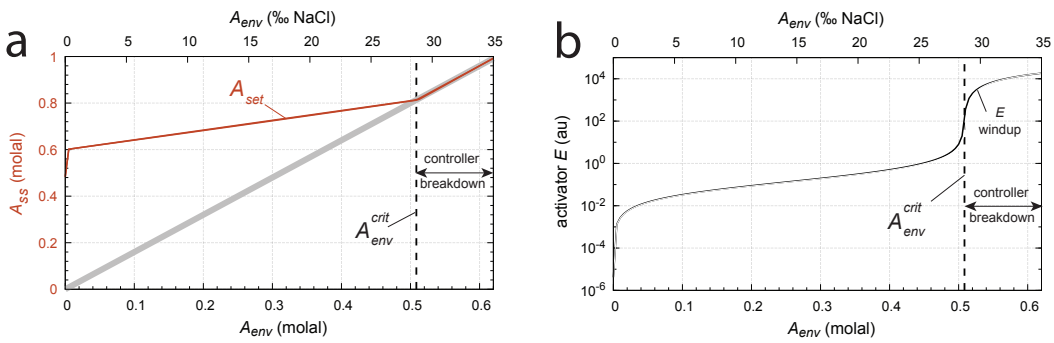

Figure 3: Enantiostasis of Fig 1 described by the negative feedback in Fig 2. Panel a: Outlined in red shows the internal (steady state) sodium ion concentration A_{ss} in dependence of environmental Na^+ concentration A_{env}. Concentration at lower abscissa is in molal, while upper abscissa is in ‰ NaCl. Vertical dashed line shows A_{env}^{crit} calculated by Eq 7. The grey thick line shows the feedback's hyper-osmotic 'line of breakdown' (see Eq 10). Panel b: E as a function of A_{env}. Rate constants: k_1=1.6×10^3, k_2=0.02, k_3=100.0, k_4=1.0×10^3, k_5=7.0, K_I=10.0, V_{max}=60.0, K_M=1.0×10^{-6}, K_a=0.1. Initial concentrations: A_0=1.0 m, E_0=0.12 au (for all A_{env}'s). Calculations were performed with a start value of $A_{env\,start}$=0.0 m and an end value of $A_{env\,end}$=0.62 m. This A_{env} range was divided into 200 A_{env} concentrations and for each A_{env} value the rate equations were solved until steady state was obtained at 2000 time units.

When $A_{env}>A_{env}^{crit}$ the compensatory flux is saturated leading to controller breakdown (Ang and McMillen, 2013). The breakdown is accompanied with positive windup of E, which means that $\dot{E}>0$ and E increases continuously. As a result, A_{ss} can no longer be kept at A_{set}. From Eq 1 the dependency of A_{ss} on A_{env} during E windup can be derived:

$$A_{ss}\,(\text{during}\,E\,\text{windup}) = \frac{k_1 A_{env}+k_2}{k_4} \tag{10}$$

which is shown by the thick grey line in Fig 3a. Note that this line is *hyper-osmotic*, because the blood sodium ion concentration A is always larger than the environmental sodium concentration A_{env}. It has a slope of about 1.6. Mangum and Towle (1977) described this line as isosmotic, which is somewhat misleading since an isosmotic line would require a slope of 1.0 with A and A_{env} being equal in concentration.

When A_{env} is zero A-inflow from another source (for example food) becomes important. In Fig 4 k_2 is stepwise increased during five phases starting with k_2=0.01 and increasing k_2 in the following phase by one order of magnitude (panel a). During the first three phases the k_2 based inflow is insufficient to keep A at A_{set} (panel b). The reason for this is that E during the first three phases is too low to keep $E/(K_M+E) \approx 1$ in order for integral control to take effect (panels c and d). First when E values have reached 10^{-3} or higher integral control becomes operative and A can be kept at A_{set}. Thus, a insufficient low activation of the NKA when crabs live in freshwater appears to be the reason that blood osmolality lies significantly below the straight red line in Fig 1 (red triangle).

At the other end we have controller breakdown when A_{set} meets the 'line of breakdown' in Fig 3. As indicated by Eqs 7, 8, and 9 breakdown occurs when inflow to A becomes too large and the compensatory flux becomes saturated. Fig 5 shows controller breakdown when either A_{env}, k_1, or k_2 exceed their critical values. In row a A_{env} is changed while the other rate parameters are kept constant. In this case A_{set} (Eq 4, orange line) changes with changed A_{env}, because A_{env} induces inhibitor I (Eq 3), which takes part in the determination of the setpoint. Once A_{env} exceeds A_{env}^{crit} (grey line) the controller breaks down and windup in E occurs. Analogous are the situations of controller breakdown when k_1 (row b) or k_2 (row c) are changed and exceed their respective critical values k_1^{crit} (Eq 8) or k_2^{crit} (Eq 9).

4. Discussion

The extrusion of sodium ions by NKA is based on a ping-pong transport mechanism known as the Albers-Post mechanism (Albers, 1967; Post et al., 1969; Jorgensen et al., 2003; Dyla et al., 2020). In the Albers-Post mechanism NKA cycles between two states, termed as E1 and E2. Fig 6a shows the mechanism in a Cleland (1963) type notation starting with the outward-facing E2 conformation with two bound potassium ions. The bind-

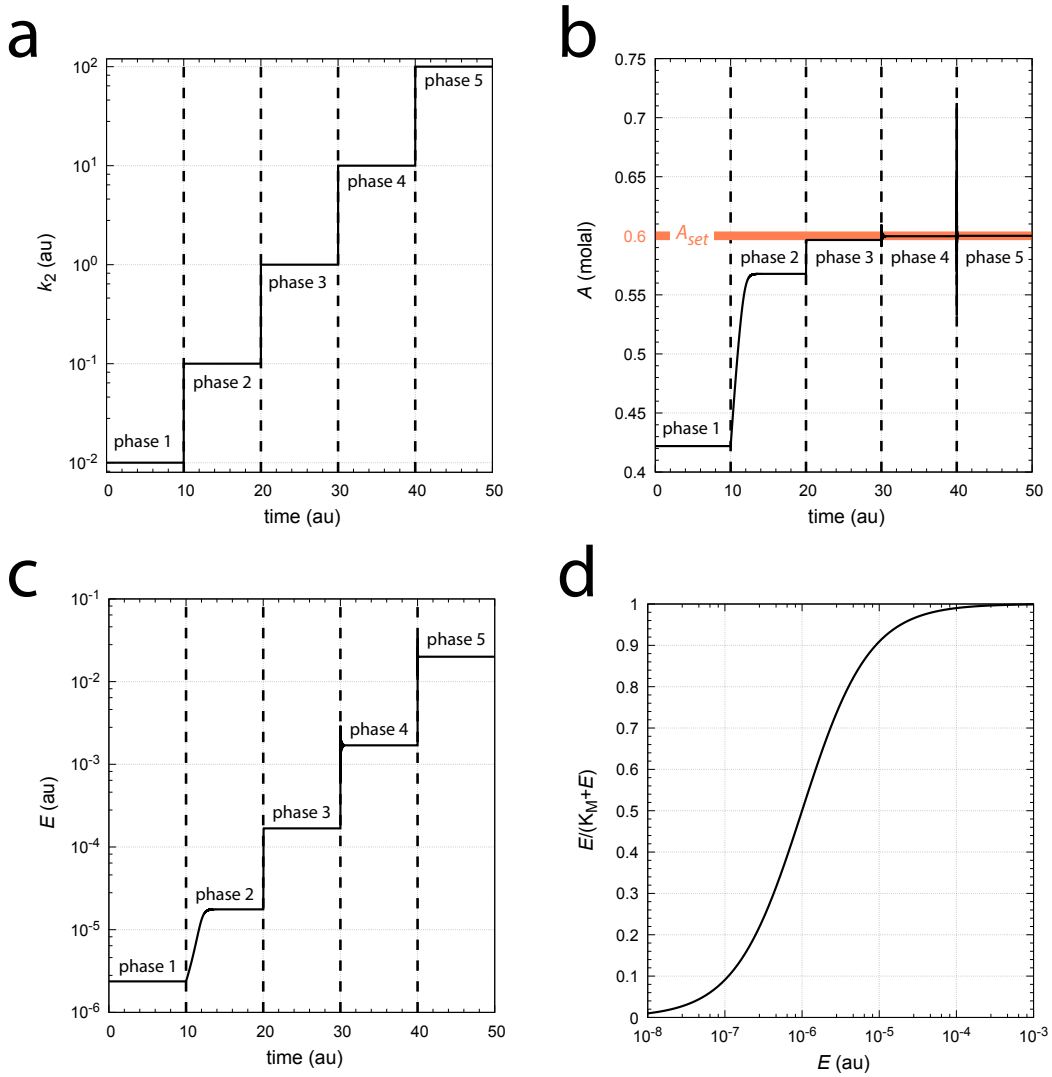

Figure 4: A sufficient A inflow is necessary to obtain homeostatic control at A_{set}. Panel a: stepwise changes of k_2 from 0.01 to 100 during 5 phases. Panel b: A as a function of time during the five phases. The setpoint A_{set}=0.6 is outlined in orange color. Panel c: E as a function of time. Panel d: Ratio $E/(K_M+E)$ as a function of E. Rate constants as in Fig 3. Initial concentrations: A_0=0.422 m, E_0=2.37·10^{-6} (au). A_{env}=0.0 m during all five phases. See Python code in supplementary material.

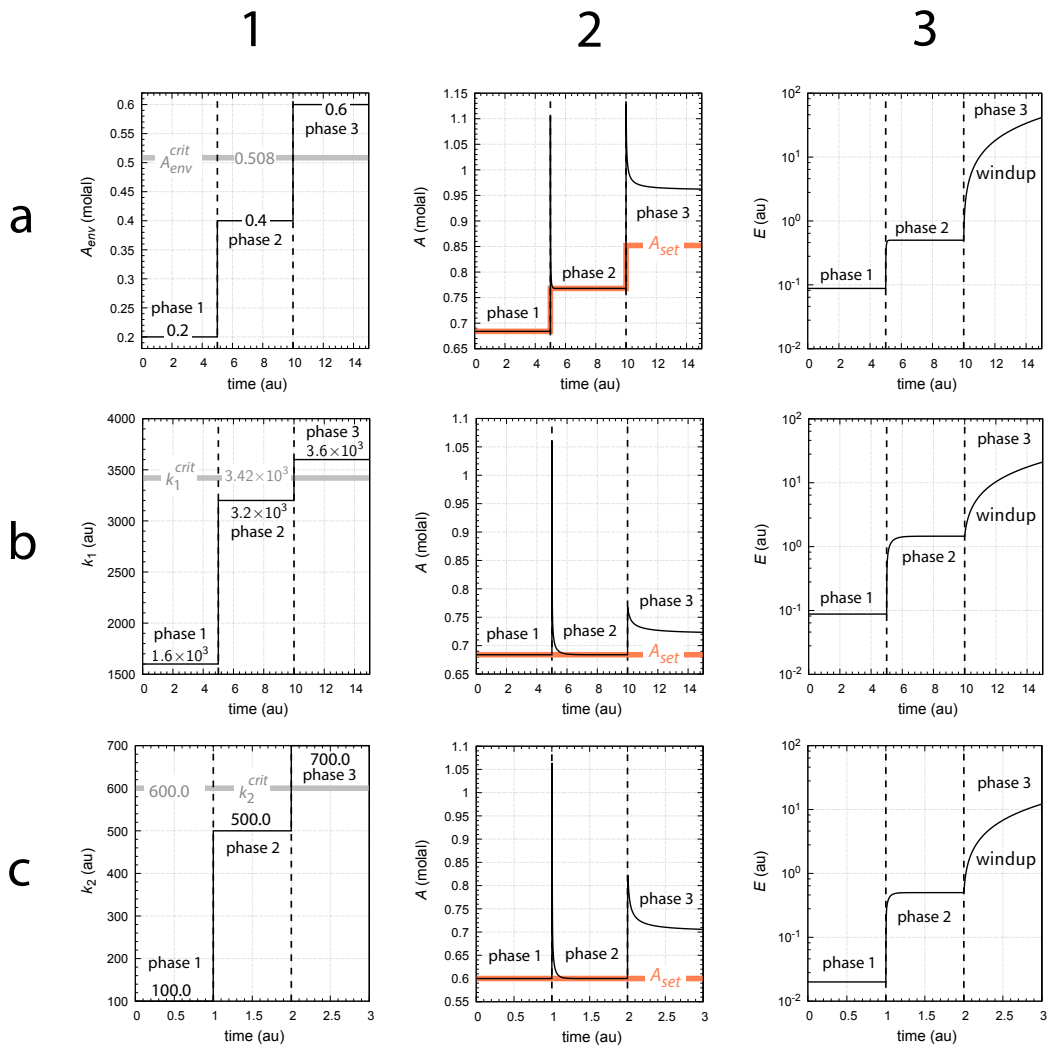

Figure 5: Controller breakdown for stepwise changes in A_{env} (row a), k_1 (row b), and k_2 (row c). Column 1 shows stepwise changes of A_{env}, k_1, and k_2 during three phases with breakdown in phase 3 when the critical values of Eqs 7, 8, or 9 (outlined as grey lines) are exceeded. Column 2 shows the resulting A's as a function of time. A_{set} is outlined in orange color. Column 3 shows the E's as a function of time. Due to the logarithmic scale the linear increase (windup) of E in phase 3 is seen as a curved increase. Other rate constants as in Fig 3. Initial concentrations, row a and b: A_0=0.684, A_{env} (row b)=0.2, E_0=0.0879; row c: A_0=0.600, E_0=0.020, A_{env}=0.0. See Python codes in Supporting Material.

ing of ATP and the presence of internal sodium ions switches to the inward facing E1 conformation with the binding of three sodium ions. This high energy conformation leads then to the ATP-driven transport of the bound sodium ions into the extracellular space. As NKA's conformation changes back into the outward facing E2 state with environmentally potassium ions bound, the cycle starts again.

The Albers-Post mechanism has been verified by several experimental methods. Using fluorescence spectroscopy and labeled NKA preparations it was found that the transition speed between E1 and E2 states depends on NKA's environment, for example whether the enzyme was reconstituted in phospholipid vesicles (Rephaeli et al., 1986) or was studied in isolation (Steinberg and Karlish, 1989). There are now more than 30 studies of NKA's crystal structure (see for example (Nyblom et al., 2013; Kanai et al., 2013; Guo et al., 2022)), which confirm the earlier anticipated (Mangum and Towle, 1977) conformational states between the outward facing E2 and the inward facing E1 forms. Molecular modeling is a useful tool as it allows to investigate conformational states that so far have escaped experimental studies (Tejral et al., 2017; Guerra et al., 2025).

However, as far as the author can see, no feedback with respect to internal sodium ion regulation by the Albers-Post mechanism has been discussed in the literature. So, how can a feedback as indicated in Fig 2 be rationalized? Fig 6b shows the suggested mechanism: In a concentration dependent manner the presence of internal sodium ion A takes part in the NKA activation and in the subsequent binding of internal Na^+ leading to the $E1{\cdot}P{\cdot}Na_3$ state. This state then switches into the outward facing E2 conformation with the release of sodium ions into the environmental (extracellular) space. The final reaction back to the $E2{\cdot}K_2$ state (outlined in blue) is described by close to zero-order kinetics where a low K_M (binding of environmental K^+ and release of P_i) will lead to integral control as described above. Thus, E in Fig 2 is identified with the activated $E1{\cdot}P{\cdot}Na_3$ form of NKA.

The mechanism shown in Fig 6b represents a short-term regulation in the sense that the increase of NKA activity when crabs move upriver into less salt-containing waters is due to a decreased NKA inhibition by environmental sodium ions. While long-term regulations of NKA via biosynthesis or turnover have been found in many cell preparations and whole animals

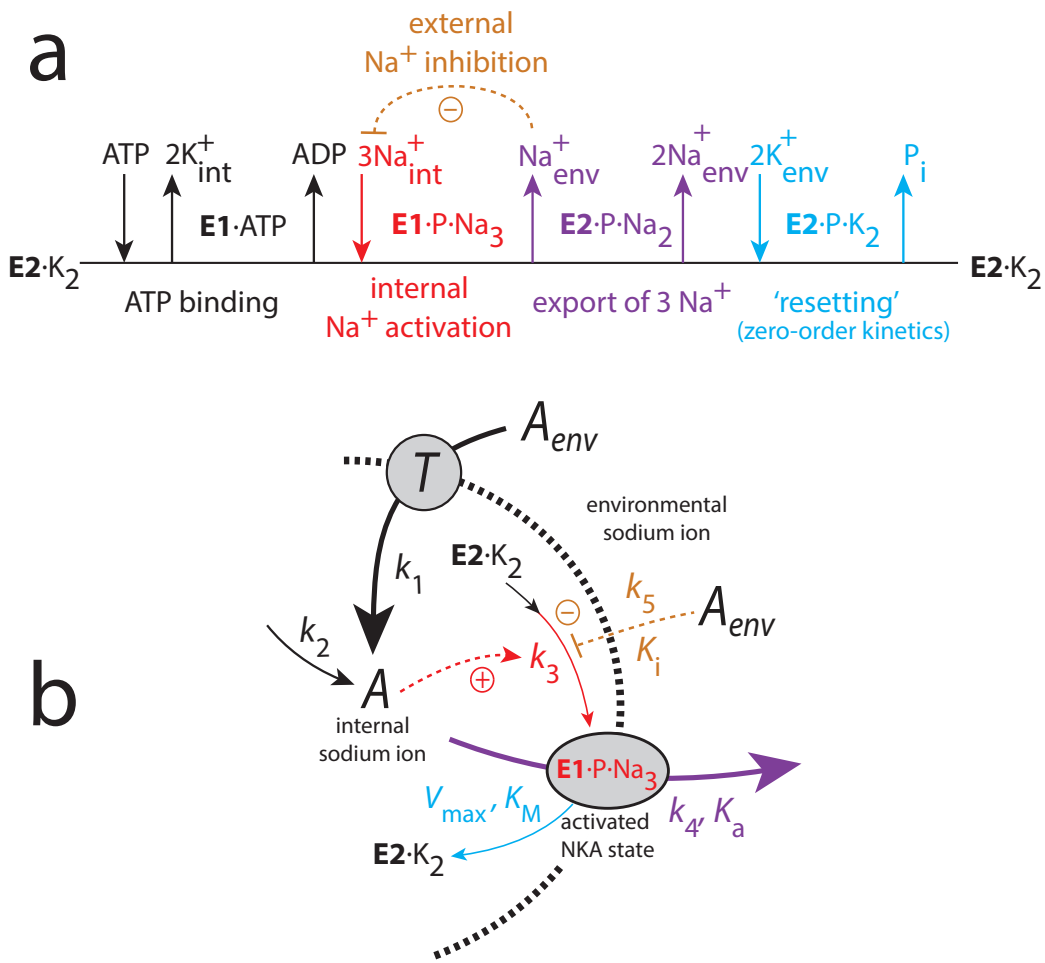

Figure 6: Mechanisms of the sodium pump and the suggested internal negative feedback. Panel a shows the Albers-Post mechanism (after Jorgensen et al. (2003)) using a Cleland (1963) type presentation. NKA switches between an E1 and E2 state. The activation and loading of the enzyme by sodium ions in the E1 state is indicated in red, while the export of sodium ions and the return to the E2 state is in violet. The 'resetting' to the starting E2·K_2 state is indicated in blue. The inhibition of NKA by external sodium ions is indicated in orange color. Panel b shows the suggested negative feedback mechanism. Other transporters, indicated by T (for example sodium-calcium exchangers NCX), pump sodium ions into the internal space, while internal sodium ions (A) activate NKA and pump them into the extracellular space (A_{env}). Coloring as in panel a. The feedback arises as A activates NKA (dashed red line), which then is pumped out (purple arrow).

(Karin and Cook, 1983), Towle et al. (2001) addressed the question whether in the blue crab the enhanced NKA activity during hyper-osmoregulation may be related to increased gene transcription and translation. The answer was negative. Changing the environmental salinity from 35 ‰ to 5‰ did not alter the mRNA and the protein of NKA in posterior gills in agreement with a reversible inhibition of NKA by environmental sodium ions.

One may wonder whether an activation of NKA by internal sodium ion is really necessary and whether a mere binding of internal sodium and its outside transport is sufficient to explain the behavior of Fig 3a. Also here the answer is negative. Since the amount of NKA is constant, as the results by Towle et al. (2001) indicate, increasing environmental sodium ions will eventually saturate NKA with the effect that the internal sodium ion concentration will increase hyperbolically enhanced by NKA's inhibition through environmental sodium ions (for details see file `No_activation.pdf` in the Supporting Material).

5. Summary and Outlook

The apparent presence of a negative feedback in the Albers-Post mechanism via an activation by internal sodium ions and their following extrusions is able to describe the blue crab's observed salinity adaption by this single feedback. While this adaptation has been suggested to be 'enantiostatic' and based on several contributing factors the here presented results show that it equally well can be described by a single homeostatic negative feedback. Thus, both enantiostasis as well as the accompanied rheostatic setpoint change can be viewed as an emergent property by a homeostatic mechanism. The view that rheostasis is an emergent property by homeostatic mechanisms became also apparent when studying the interaction between two combined homeostatic controllers (Ruoff, 2025). There, rheostatic changes are observed when homeostasis by one controller is gradually replaced by the control through another feedback.

The here suggested internal feedback within the Albers-Post mechanism appears to apply also to other pumps based on this mechanism, such as the Ca pump SERCA is activated by calcium (Espinoza-Fonseca and Thomas,

2011; Dyla et al., 2020). In this respect, homeostatic regulations may already occur by intrinsic negative feedback within these pumps.

Glossary

Controlled variable: The variable which is under homeostatic control with one or several setpoints.

Controller variable or manipulated variable: The controller or manipulated variable generates a compensatory flux to oppose a perturbation applied to the controlled variable.

Integral control (integral feedback): In integral control (integral feedback) the controller variable and its compensatory flux is related to the integrated error of the controller, i.e. the integrated difference between the actual value of the controlled variable and the controller's setpoint. Integral feedback leads to perfect adaptation to a controller's setpoint. Different kinetic mechanisms can result in integral control.

Windup: The continuous increase or decrease of a controller variable.

NKA: Na-K ATPase, sodium pump.

Supporting Material

Python: Python code showing the results of Fig 3 (`Fig3.py`), Fig 4 (`Fig4.py`), and the results of rows a, b, c in Fig 5 (`Fig5a.py`, `Fig5b.py`, `Fig5c.py`). Besides Python (`https://www.python.org`), Numpy (`https://numpy.org`), Matplotlib (`https://matplotlib.org`), and Scipy (`https://scipy.org`) need to be installed. The scripts can be run via the Terminal (Linux, Unix, Mac OSX) or the Command Prompt (Windows) by using the command '`python name.py`', where '`name`' is the name of the python file.

`No-feedback.pdf`**:** The file describes the hyperbolic increase of internal sodium ion concentrations upon increased A_{env} levels when the negative feedback by pump activation is absent.

Funding sources

This research did not receive any specific grant from funding agencies in the public, commercial, or not-for-profit sectors.

References

Albers, R., 1967. Biochemical aspects of active transport. Annual Review of Biochemistry 36, 727–756.

Ang, J., McMillen, D., 2013. Physical constraints on biological integral control design for homeostasis and sensory adaptation. Biophys J 104, 505–15.

Aoki, S.K., Lillacci, G., Gupta, A., Baumschlager, A., Schweingruber, D., Khammash, M., 2019. A universal biomolecular integral feedback controller for robust perfect adaptation. Nature 570, 533–537.

Briat, C., Gupta, A., Khammash, M., 2016. Antithetic integral feedback ensures robust perfect adaptation in noisy biomolecular networks. Cell Systems 2, 15–26.

Cannon, W., 1929. Organization for Physiological Homeostasis. Physiol. Rev. 9, 399–431.

Clancy, J., McVicar, A.J., 2002. Physiology and Anatomy. A Homeostatic Approach. Second edition. Hodder Arnold Publication, London, UK.

Cleland, W.W., 1963. The kinetics of enzyme-catalyzed reactions with two or more substrates or products: I. Nomenclature and rate equations. Biochimica et Biophysica Acta (BBA)-Specialized Section on Enzymological Subjects 67, 104–137.

Drengstig, T., Jolma, I., Ni, X., Thorsen, K., Xu, X., Ruoff, P., 2012. A Basic Set of Homeostatic Controller Motifs. Biophys J 103, 2000–2010.

Drengstig, T., Ni, X., Thorsen, K., Jolma, I., Ruoff, P., 2012. Robust adaptation and homeostasis by autocatalysis. J Phys Chem B 116, 5355–5363.

Dyla, M., Kjærgaard, M., Poulsen, H., Nissen, P., 2020. Structure and mechanism of P-type ATPase ion pumps. Annual Review of Biochemistry 89, 583–603.

Espinoza-Fonseca, L.M., Thomas, D.D., 2011. Atomic-level characterization of the activation mechanism of SERCA by calcium. PLoS One 6, e26936.

Fjeld, G., Thorsen, K., Drengstig, T., Ruoff, P., 2017. Performance of homeostatic controller motifs dealing with perturbations of rapid growth and depletion. J Phys Chem B 121, 6097–6107.

Garrahan, P., Glynn, I., 1967. The sensitivity of the sodium pump to external sodium. The Journal of Physiology 192, 175–188.

Guerra, J., Rui, H., Roux, B., 2025. Multistate kinetic model of the sodium–potassium atpase. The Journal of Physical Chemistry B 129, 9609–9621.

Guo, Y., Zhang, Y., Yan, R., Huang, B., Ye, F., Wu, L., Chi, X., Shi, Y., Zhou, Q., 2022. Cryo-em structures of recombinant human sodium-potassium pump determined in three different states. Nature Communications 13, 3957.

Hochachka, P.W., Somero, G.N., 1984. Biochemical Adaptation. Princeton University Press, Princeton, New Jersey.

Jorgensen, P.L., Håkansson, K.O., Karlish, S.J., 2003. Structure and mechanism of Na,K-ATPase: Functional sites and their interactions. Annual Review of Physiology 65, 817–849.

Kanai, R., Ogawa, H., Vilsen, B., Cornelius, F., Toyoshima, C., 2013. Crystal structure of a Na^+-bound Na^+,K^+-ATPase preceding the E1P state. Nature 502, 201–206.

Kaplan, J.H., 1982. Sodium pump-mediated ATP: ADP exchange. The sided effects of sodium and potassium ions. The Journal of General Physiology 80, 915–937.

Karin, N.J., Cook, J.S., 1983. Regulation of Na,K-ATPase by Its Biosynthesis and Turnover. Current Topics in Membranes and Transport 19, 713–751.

Khammash, M.H., 2021. Perfect adaptation in biology. Cell Systems 12, 509–521.

Langley, L.L., 1973. Homeostasis. Origins of the Concept. Dowden, Hutchinson & Ross, Inc., Stroudsbourg, Pennsylvania.

Mangum, C., Towle, D., 1977. Physiological adaptation to unstable environments: Inconstancy of the internal milieu in an animal may be a regulatory mechanism. American Scientist 65, 67–75.

Mrosovsky, N., 1990. Rheostasis. The Physiology of Change. Oxford University Press, New York.

Ni, X., Drengstig, T., Ruoff, P., 2009. The control of the controller: Molecular mechanisms for robust perfect adaptation and temperature compensation. Biophys J 97, 1244–53.

Nyblom, M., Poulsen, H., Gourdon, P., Reinhard, L., Andersson, M., Lindahl, E., Fedosova, N., Nissen, P., 2013. Crystal structure of Na^+,K^+-ATPase in the Na^+-bound state. Science 342, 123–127.

Post, R., Kume, S., Tobin, T., Orcutt, B., Sen, A., 1969. Flexibility of an active center in sodium-plus-potassium adenosine triphosphatase. The Journal of General Physiology 54, 306–326.

Radhakrishnan, K., Hindmarsh, A., 1993. Description and Use of LSODE, the Livermore Solver for Ordinary Differential Equations. NASA Reference Publication 1327, Lawrence Livermore National Laboratory Report UCRL-ID-113855. National Aeronautics and Space Administration, Lewis Research Center, Cleveland, OH 44135-3191.

Rephaeli, A., Richards, D., Karlish, S., 1986. Conformational transitions in fluorescein-labeled (Na, K) ATPase reconstituted into phospholipid vesicles. Journal of Biological Chemistry 261, 6248–6254.

Ruoff, P., 2025. Flux organizations and control modes in antagonistically combined negative feedback loops. bioRxiv doi:10.1101/2025.11.09.687434.

Sachs, J., 1977. Kinetics of the inhibition of the Na-K pump by external sodium. The Journal of Physiology 264, 449–470.

Shoval, O., Goentoro, L., Hart, Y., Mayo, A., Sontag, E., Alon, U., 2010. Fold-change detection and scalar symmetry of sensory input fields. PNAS 107, 15995–16000.

Skou, J.C., Esmann, M., 1992. The Na,K-ATPase. Journal of Bioenergetics and Biomembranes 24, 249–261.

Steinberg, M., Karlish, S., 1989. Studies on conformational changes in Na, K-ATPase labeled with 5-iodoacetamidofluorescein. Journal of Biological Chemistry 264, 2726–2734.

Stevenson, T.J., 2024. On Rheostasis. The Hierarchical Organization of Physiological Stability. Oxford University Press, New York.

Tejral, G., Sopko, B., Necas, A., Schoner, W., Amler, E., 2017. Computer modelling reveals new conformers of the ATP binding loop of Na^+/K^+-ATPase involved in the transphosphorylation process of the sodium pump. PeerJ 5, e3087.

Towle, D.W., Paulsen, R.S., Weihrauch, D., Kordylewski, M., Salvador, C., Lignot, J.H., Spanings-Pierrot, C., 2001. Na^++K^+-ATPase in gills of the blue crab *Callinectes sapidus*: cDNA sequencing and salinity-related expression of α-subunit mRNA and protein. Journal of Experimental Biology 204, 4005–4012.

Waheed, Q., Zhou, H., Ruoff, P., 2022. Kinetics and mechanisms of catalyzed dual-E (antithetic) controllers. PLoS One 17, e0262371.

Wilkie, J., Johnson, M., Reza, K., 2002. Control Engineering. An Introductory Course. Palgrave, New York.

Yi, T., Huang, Y., Simon, M., Doyle, J., 2000. Robust perfect adaptation in bacterial chemotaxis through integral feedback control. PNAS 97, 4649–53.